Lowess algorithm of GeneSpring version 7 (Agilent Technologies). Spots with a signal/background ratio <2.0 in at least five of seven experiments were excluded from the data analysis. Finally, 16,555 genes were selected and analyzed. The expression level of each gene was represented as the relative value to the control.

Western Blotting

Antibodies used for Western blotting (19) were anti-actin monoclonal antibody (A2066, Sigma-Aldrich), anti-β-catenin monoclonal antibody (610153, BD Biosciences, San Jose, CA), anti-cyclin D1 (M20), c-Myc (9E10), Ki-ras [K-Ras-2B (C-19)], and p53 (FL393) monoclonal antibodies (Santa Cruz Biotechnology, Inc., Santa Cruz, CA), and an anti-c-ErbB-2 monoclonal antibody (A0485, DakoCytomation Denmark A/S, Glostrup, Denmark).

Animal Experiments

Inbred mouse strain, C57BL/6J, was obtained from CLEA Japan, Inc. (Tokyo, Japan) and fed with 5 g/d high fat diet (HFD32, CLEA Japan) mixed with 0.1% GO-Y030 or GO-Y031 (w/w). Animal experiments were done following approval from institutional guideline.

Results

Screening of Phytochemical Analogues

Dietary phytochemicals, including curcumin, resveratrol, capsaicin, caffeic acid phenethyl ester, [6]-gingerol, diallyl sulfide, epigallocatechin-3-gallate, and indole-3-carbinol, are known to have both growth-suppressive and chemopreventive activity against specific types of cancers (1). From our synthetic organic compound library composed of >2,000 species, we selected 45 compounds structurally analogous to the phytochemicals mentioned above and tested their abilities to suppress the growth of the colon cancer cell line DLD-1. Only one compound, GO-035, which is nominated as an analogue of curcumin, was found to have a stronger ability to suppress the growth of DLD-1 compared with curcumin (Figs. 1A and 2A). The IC_{50} value of GO-035 was 2.0 μmol/L, a value four times lower than that of curcumin (IC_{50}, 8.0 μmol/L; Fig. 2A). The growth-suppressive activity of GO-035 in two other colon cancer cell lines, SW620 and HCT116 cells ($p53^{+/+}$), was also examined (Fig. 2B and C). In these cases, both the IC_{50} values of GO-035 were again lower than that of curcumin. The IC_{50} values of GO-035 in SW620 and HCT116 cells ($p53^{+/+}$) were 3.5 and 1.6 μmol/L, respectively, and those of curcumin were 10.0 and 6.5 μmol/L, respectively. The growth-suppressive activity of GO-035 was examined in other cancer cell lines, including lines derived from stomach (GCIY, SH10TC), lung (LK87), breast (MCF7), ovary (OVK18), prostate (PC3), pancreas (PK9), bile duct (HuCCT1), thyroid gland (8505c), skin (A431), kidney (ACHN), and liver cancers (HepG2) and also melanoma (G361; Fig. 3A). Curcumin exhibited growth-suppressive activity in all the types of cancer cell lines tested. The IC_{50} values of curcumin ranged from 4.0 to 9.0 μmol/L in the cell lines tested, whereas those of GO-035 ranged from 0.6 to 7.0 μmol/L. GO-035 exhibited 2.3 to 10.0 times more

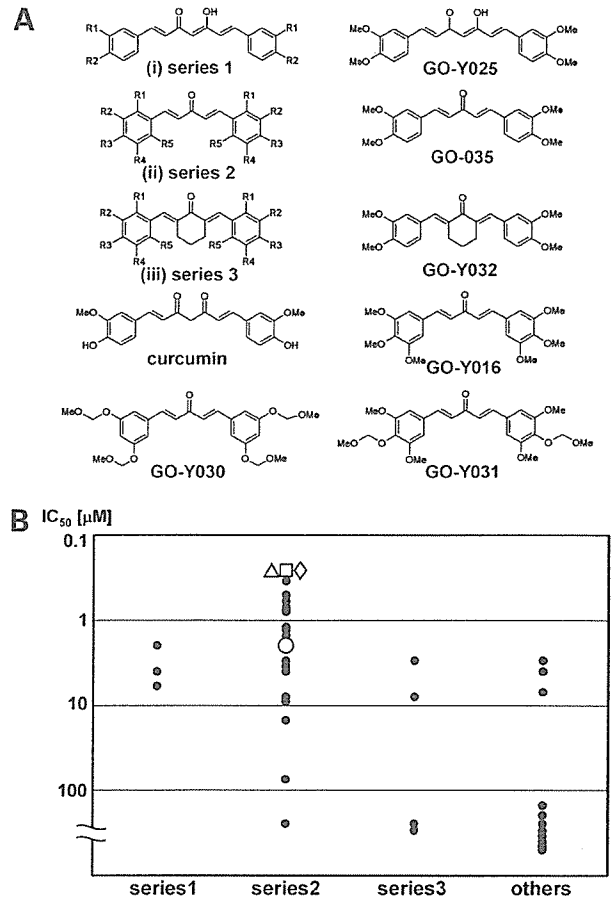

Figure 1. Structures of new curcumin analogues and their abilities to induce cell growth suppression. **A**, common structures of three series of curcumin analogues. **B**, IC_{50} values of the new curcumin analogues against HCT116 cells ($p53^{+/+}$). ○, GO-035; ◇, GO-Y016; □, GO-Y030; Δ, GO-Y031.

growth-suppressive activity in HCT116 cells ($p53^{+/+}$), SW620, GCIY, LK87, MCF7, PK9, 8505c, and G361 than curcumin in the same cell lines at the concentrations tested (Fig. 3A).

Growth-Suppressive Potential of New Curcumin Analogues

A panel of related compounds was also synthesized and examined. Four series of curcumin analogues were designed and synthesized aiming not only to identify crucial structural motifs leading to growth-suppressive ability for carcinogenesis but also to gain insight into directions for designing new derivatives with increased activities: (*a*) curcumin-type compounds that retain the 7-carbon spacer between the aryl rings (diarylheptanoids), (*b*) GO-035-type compounds that have a 5-carbon spacer between the aryl rings (diarylpentanoids), (*c*) GO-035-type compounds in which conformational freedom is fixed by the central cyclic ketone structure, and (*d*) others (Fig. 1B; Supplementary Fig. S2; Supplementary Table S1).[5] Results

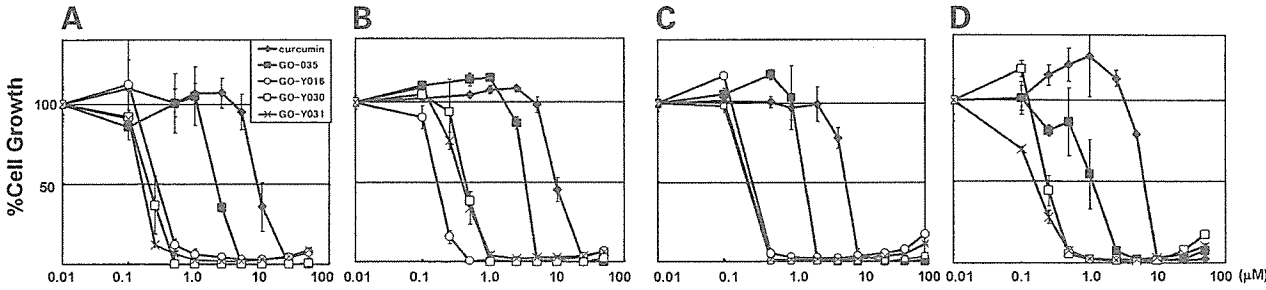

Figure 2. Growth-suppressive potentials of the new curcumin analogues. Growth suppression by curcumin and its analogues. **A,** DLD-1. **B,** SW620. **C,** HCT116 cells ($p53^{+/+}$). **D,** HCT116 cells ($p53^{-/-}$). The percentage of growth in the control cell line treated with 1% DMSO alone was calculated. *Points,* mean of triplicate experiments; *bars,* SD.

during the course of this study suggested that (*a*) the methyl modification of the *p*-hydroxy group relative to the α,β-unsaturated ketone moiety leads to considerable enhancement in the growth-suppressive activity (e.g., GO-Y025 > curcumin), (*b*) a 5-carbon tether is superior to a 7-carbon tether (e.g., GO-035 > GO-025), and (*c*) conformational fixation around the enone subunit leads to significant attenuation of the activity (e.g., GO-035 ≫ GO-032; Fig. 1A and B). Hence, derivatives in series 2 were synthesized to identify new compounds with enhanced activity. Fifty-one compounds, including 33 diarylpentanoids, were newly synthesized and their growth-suppressive effect on HCT116 cells ($p53^{+/+}$) was examined (Fig. 1B; Supplementary Table S1).[5] The IC_{50} values of series 2 compounds ranged from 0.25 to over 100 μmol/L (Fig. 1B; Supplementary Table S1).[5] Among them, 34 compounds showed a higher potential to suppress growth in HCT116 cells ($p53^{+/+}$) compared with curcumin, and 18 of the 34 compounds showed higher growth-suppressive activity compared with GO-035. These compounds had 1,5-diarylpentadienone skeleton as the common structural motif, and it was indicated that the introduction of suitable alkoxy groups on the aromatic rings led to an increase in the growth-suppressive potential. Among the diarylpentanoids, compounds GO-Y016, GO-Y030, and GO-Y031 showed the highest growth-suppressive activity in HCT116 cells ($p53^{+/+}$). The IC_{50} value of these three compounds was 0.25 μmol/L (Fig. 2; Supplementary Table S1).[5] This low value corresponded to 1/32 of the IC_{50} value of curcumin and 1/8 that of GO-035. The IC_{50} values of GO-Y016 in all the cell lines tested ranged from 0.10 to 0.50 μmol/L, except A431 and HepG2, where the IC_{50} value was 2.0 μmol/L in each case (Fig. 3A). GO-Y016 exhibited 12 to 60 times higher growth-suppressive activity than the highest activities of curcumin. GO-Y016 exhibited 4.8 to 18.0 times higher growth-suppressive activity compared with GO-035. Similar growth suppression activities were observed for both GO-Y030 and GO-Y031 (Fig. 3A). GO-Y030 exhibited 8.0 to 40.0 times and GO-Y031 exhibited 13.2 to 50.0 times higher growth-suppressive activities compared with curcumin in the cell lines where growth suppression occurred. Compared with GO-035, GO-Y030 exhibited 3.0 to 13.5 times and GO-Y031 exhibited 3.0 to 23.3 times the growth-suppressive activity (Fig. 3A). Each of the compounds GO-Y016, GO-Y030, and GO-Y031 had fundamentally stronger growth suppression activities in cancer cell lines than curcumin or GO-035.

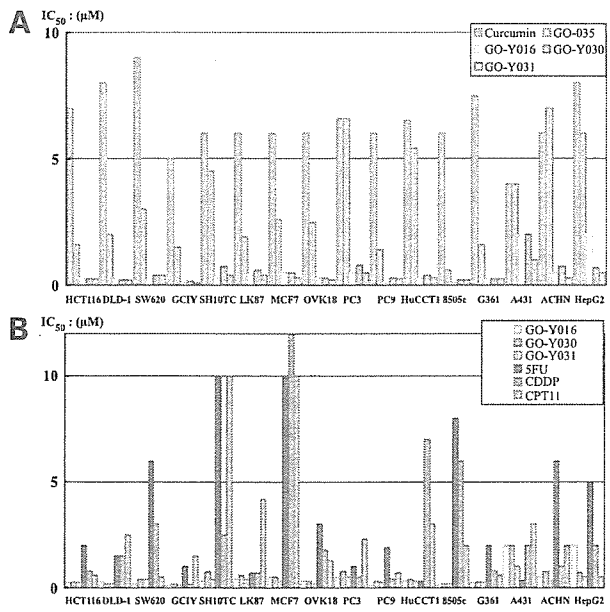

Figure 3. Growth-suppressive abilities of the new curcumin analogues. **A,** growth suppression of various types of cancer cell lines. **B,** comparison of growth suppression with anticancer agents. The origins of cancers are indicated below the name of the cell lines. *Ova,* ovary; *Panc,* pancreas.

Growth-Suppressive Activities of New Curcumin Analogues Compared with Currently Used Anticancer Drugs

We compared the growth-suppressive activities of GO-Y016, GO-Y030, and GO-Y031 with the most commonly used chemotherapeutic agents [i.e., 5-fluorouracil (5-FU), CDDP, and CPT-11]. IC_{50} values of 5-FU on 16 cancer cell lines ranged from 0.35 to 10.0 μmol/L (Fig. 3B). Comparison of the growth-suppressive potential between 5-FU and these three diarylpentanoids was carried out by calculating the ratio of IC_{50} value of 5-FU to that of diarylpentanoid

[IC_{50} ratio (5-FU/diarylpentanoid)]. In LK87, PC3, HuCCT1, and A431, there was no apparent difference between the growth-suppressive activities of 5-FU and the diarylpentanoids. The IC_{50} ratios (5-FU/diarylpentanoid) in the other 12 cell lines ranged from 6.0 to 80.0, except for the IC_{50} ratio (5-FU/GO-Y016) in cell line HepG2 (2.5 μmol/L). GO-Y016, GO-Y030, and GO-Y031 were able to induce a stronger growth suppression at a much lower concentration than 5-FU in the majority of cancer cell lines. The IC_{50} values of CDDP on 16 cell lines ranged from 0.16 to 17.0 μmol/L. In cell lines GCIY, LK87, PC3, and PK9, the IC_{50} values ranged from 0.16 to 0.7 μmol/L. They were relatively sensitive to CDDP. The IC_{50} ratios (CDDP/diarylpentanoid) in MCF7, HuCCT1, and 8505c ranged from 17.5 to 60.0, indicating that GO-Y016, GO-Y030, and GO-Y031 could induce stronger growth suppression at a concentration lower than that of CDDP in some types of cancer. The IC_{50} values of CPT-11 on 16 cell lines ranged from 0.5 to 10.0 μmol/L. The IC_{50} ratio (CPT-11/diarylpentanoid) of DLD-1, SH10TC, MCF7, and 8505c ranged from 10.0 to 33.3, indicating that GO-Y016, GO-Y030, and GO-Y031 could induce stronger growth suppression at a concentration lower than that of CPT-11 in some types of cancer.

The Effect of New Curcumin Analogues on Cell Cycle Progression

The effect of each diarylpentanoids on cell cycle progression was examined by fluorescence-activated cell sorting analysis (Fig. 4). HCT116 cells ($p53^{+/+}$) were treated with curcumin, GO-035, GO-Y016, GO-Y030, and GO-Y031. The concentrations of compounds were chosen from the growth suppression experiments showing moderate toxicity. As shown in Fig. 4, 30 hours of treatment induced a significant effect in each experiment. As shown previously (10), 52% of the cell population arrested in the G_2-M phase at 20 μmol/L curcumin. Conversely, the cell population at the G_0-G_1 phase was reduced to 7% probably due to the G_2-M arrest, but the S phase fraction did not change. GO-035 treatment at 5 μmol/L had the same effect on cell cycle progression, where 47% of the cell population arrested in the G_2-M phase, and the G_0-G_1 phase fraction was reduced to 7%. The S phase fraction did not change at 5 μmol/L GO-035 treatment. On the other hand, GO-Y016, GO-Y030, and GO-Y031, which have the highest growth-suppressive activities among the diarylpentanoids, exerted different effects on cell cycle progression. GO-Y016 was difficult to dissolve; thus, only 1 μmol/L could be assessed. For 1 μmol/L GO-Y016, the same degree of G_2-M arrest was observed as seen in 20 μmol/L curcumin. G_2-M arrest was also observed with 2 μmol/L GO-Y030 and GO-Y031 treatment. The most drastic change with GO-Y016 was the reduction of the S phase fraction to 28% of the cell population, whereas the S phase fraction of the control, curcumin, and GO-035 was 46%, 41%, and 46%, respectively. This tendency was more apparent in the cases of 2 μmol/L GO-Y030 and GO-Y031 treatment, where the reduction of the S phase fraction was 15% and 10%, respectively. Furthermore, the sub-G_1 fraction (20% and 26% of the cell population) additionally appeared following GO-Y030 and GO-Y031 treatment, respectively. The reduction of the S phase fraction corresponded to the inhibition of DNA synthesis, whereas the elevation of the sub-G_1 fraction corresponded to the induction of apoptosis. We suggest that the activities of GO-Y030 and GO-Y031 were reinforced in these two aspects.

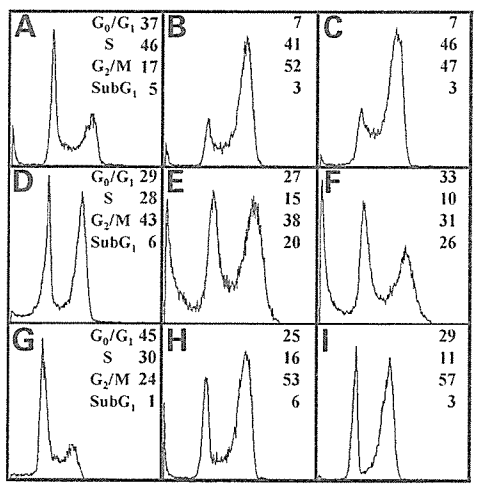

Figure 4. Effects of the new curcumin analogues on cell cycle progression. Cell cycle profile of HCT116 cells ($p53^{+/+}$) treated with curcumin. *Inset*, percentage of cells in G_0-G_1, S, G_2-M, and sub-G_1 phases. **A**, control (1% DMSO). **B**, curcumin (20 μmol/L). **C**, GO-035 (5 μmol/L). **D**, GO-Y016 (1 μmol/L). **E**, GO-Y030 (2 μmol/L). **F**, GO-Y031 (2 μmol/L). **G**, Z-DEVD-fmk (20 μmol/L). **H**, GO-Y030 (2 μmol/L) + Z-DEVD-fmk (20 μmol/L). **I**, GO-Y031 (2 μmol/L) + Z-DEVD-fmk (20 μmol/L).

Caspase-3-Like Activity with the New Curcumin Analogues

The induction of caspase-3-like activity with new curcumin analogues was examined. Caspase-3 is one of the major components of the apoptosis pathway, including curcumin-related apoptosis. Caspase-3-like activity was measured by measuring the concentration of 7-amido-4-methylcoumarin generated by cleavage following treatment with curcumin and its new analogues. New curcumin analogues, such as GO-035 (5 μmol/L), GO-Y016 (2.5 μmol/L), GO-Y030 (2.5 μmol/L), and GO-Y031 (2.5 μmol/L), showed 67.38 ± 1.03, 56.93 ± 3.35, 81.45 ± 5.29, and 67.33 ± 3.30 arbitrary fluorescent units/min/mg caspase-3-like activities that are 1.33, 1.12, 1.61, and 1.33 times higher than 20 μmol/L curcumin treatment, respectively (curcumin, 50.69 ± 1.16 arbitrary fluorescent units/min/mg; Supplementary Fig. S3).[5] We found that the new curcumin analogues are slightly superior to curcumin with respect to caspase-3-like activities. However, fluorescence-activated cell sorting analysis clearly indicated that the treatment with caspase-3/caspase-8 inhibitor Z-DEVD-fmk reduced the sub-G_1 fraction to the basal level in either case of GO-Y030 or GO-Y031 (Fig. 4H and I). Conversely, G_2-M arrest was not released in either case when treated with Z-DEVD-fmk (Fig. 4H and I).

Effects of New Curcumin Analogues on Gene Expression

Much is known about the effects of curcumin on gene expression at the transcriptional and posttranscriptional level (4, 9, 10, 21). The suppression of NF-κB transactivation is one of the biological effects by curcumin. The relative level of NF-κB transactivation was 0.24 ± 0.02 at 20 μmol/L curcumin treatment, whereas they were 0.59 ± 0.07 and 0.53 ± 0.07 at 2.5 μmol/L GO-Y030 and GO-Y031 treatment, respectively (Supplementary Fig. S4).[5] Suppression of NF-κB transactivation was observed in a dose-dependent manner for curcumin. On the other hand, the extent of suppression was rather weak with GO-Y030 and GO-Y031 even at the concentration where the biological effect was apparent. These results indicate that the suppression of NF-κB transactivation is not directly involved in the enhancement of growth-suppressive activities seen in the new curcumin analogues. Then, the comprehensive expression profiling affected with these compounds was estimated by using microarray analysis. Almost curcumin-related genes described in the literature were spotted within 2-fold variation compared with curcumin when treated with GO-Y030 or GO-Y031 (Supplementary Fig. S5A and B).[5] Among them, the expression levels of the target genes of NF-κB transactivation were not always suppressed, rather stable with few exceptions, such as *Bcl-2* in GO-Y030 or *c-Myc* in GO-Y031 cases (Supplementary Fig. S5C).[5] The expression level of *β-catenin* was stable after the treatment of these compounds. On the other hand, the expression levels of several other genes, including *ErbB-2* and *Ki-ras*, were down-regulated when treated with curcumin and its analogues, whereas the level of *TP53* was up-regulated in the cases of GO-Y030 and GO-Y031 (Supplementary Fig. S5D).[5] To validate the effect on the expression levels of these oncoproteins with the new curcumin analogues, Western blot analyses was carried out. ErbB-2 expression completely disappeared with each treatment of 5 μmol/L GO-035, 2.5 μmol/L GO-Y030, and 2.5 μmol/L GO-Y031 as well as 20 μmol/L curcumin (Fig. 5A). c-Myc expression was down-regulated to 50% of control with each treatment of 5 μmol/L GO-035 and 2.5 μmol/L GO-Y030 as well as 20 μmol/L curcumin, except 2.5 μmol/L GO-Y031 treatment where the reduction of c-Myc expression was 80% of control. Cyclin D1 expression was maximally down-regulated by 5 μmol/L GO-035 and 2.5 μmol/L GO-Y030 treatments to 30% of control. GO-Y031 (2.5 μmol/L) and curcumin (20 μmol/L) down-regulated the gene to a lesser extent to 60% and 80% of control, respectively. In the cases of c-Myc and cyclin D1, the transcriptional levels of these genes were stable, but they were down-regulated at the protein level. Curcumin is also well studied to induce the degradation of β-catenin. Similar levels of β-catenin degradation were observed at 5 μmol/L GO-035, 2.5 μmol/L GO-Y030, and GO-Y031 treatment as well as 20 μmol/L curcumin treatment (Fig. 5B). The expression level of Ki-ras was reduced with curcumin as well as its new analogues, those were reduced to 30%, 20%, 20%, and 50% of control in 20 μmol/L curcumin, 5 μmol/L GO-035, 2.5 μmol/L GO-Y030, and GO-Y031 treatments, respectively (Fig. 5B). This is the first evidence that curcumin and its analogues successfully induced the reduction of the activated *Ki-ras* in the colorectal cancer cell line (22). Previously, it has been

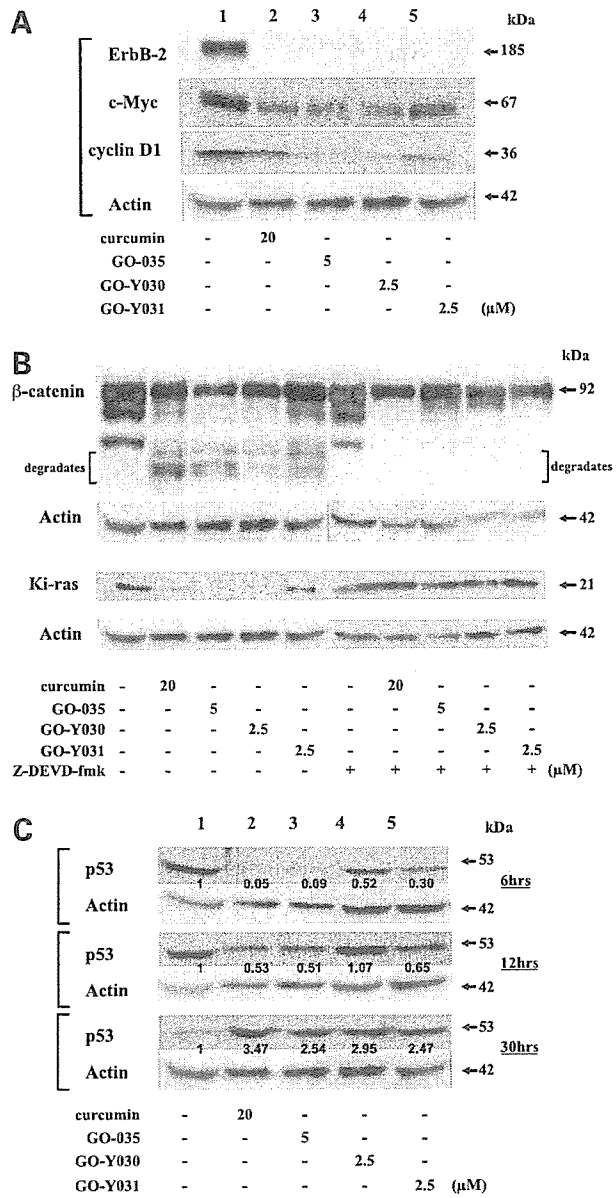

Figure 5. Western blot analyses of the genes affected with the new curcumin analogues. **A,** protein levels of ErbB-2, c-Myc, and cyclin D1 affected with curcumin and its analogues in HCT116. **B,** expression of β-catenin and Ki-ras with curcumin and its analogues. HCT116 cells ($p53^{+/+}$) were treated with the compounds at the indicated concentrations for 30 h with (*lanes 6 – 10*) or without (*lanes 1 – 5*) Z-DEVD-fmk pretreatment. *Bracket,* β-catenin breakdown products. **C,** stability of p53 treated with the new curcumin analogues. The stability of p53 was examined 6, 12, and 30 h after exposure. Quantification of each expression level was carried out by Image Gauge version 3.0 (Fuji Photo Film) standardized by the value of β-actin (*Actin*) and represented as a relative value to the control (1% DMSO alone; *lane 1*). *Arrows,* protein sizes.

shown that caspase-3 inhibition blocked β-catenin degradation with curcumin and that caspase-3 plays a crucial role in curcumin-induced β-catenin degradation but neither proteasomal nor lysosomal pathway (10). To examine the involvement of caspase-3 in β-catenin degradation as well as Ki-ras, cyclin D1, and c-Myc with the new curcumin analogues, Z-DEVD-fmk was applied. Pretreatment of 20 μmol/L Z-DEVD-fmk completely blocked the β-catenin degradation with GO-035, GO-Y030, and GO-Y031 as well as curcumin (Fig. 5B). The down-regulation of Ki-ras expression with curcumin, GO-035, GO-Y030, and GO-Y031 was also completely blocked by Z-DEVD-fmk treatment (Fig. 5B). The down-regulation of ErbB-2, c-Myc, and cyclin D1 was not completely blocked by Z-DEVD-fmk treatment (data not shown). The protein level of p53 with curcumin seems to depend on the cell types, which is overexpressed in some cell types and down-regulated in the others (23–25). We examined the effect of the new curcumin analogues on p53 expression level in HCT116 cells ($p53^{+/+}$) as well as curcumin (Fig. 5C). Curcumin reduced the expression level of p53 to 5% of control during the first 6 hours after exposure, and then the expression level gradually recovered (Fig. 5C). However, for GO-Y030, p53 was relatively stable and its level was reduced to as low as 40% of control during the first 6 hours. For GO-Y031, the result was between that of curcumin and GO-Y030. After the temporal reduction, overexpression of p53 was observed in all cases of curcumin analogues at 30 hours after exposure (Fig. 5C). As shown above, the trancriptional, posttranscriptional, or both mechanisms regulate the gene expression affected by curcumin and its analogues. The regulatory mechanisms varied individually among the genes. To examine the biological significance of the overexpression of p53, we compared the IC_{50} values of GO-Y030 between HCT116 cells ($p53^{+/+}$) and HCT116 cells ($p53^{-/-}$). The IC_{50} values of HCT116 cells ($p53^{+/+}$) and HCT116 cells ($p53^{-/-}$) were 0.18 and 0.23 μmol/L, respectively (Fig. 2A and D). It was considered that there was no relationship between p53 overexpression and the enhanced apoptosis with GO-Y030. The biological significance of p53 overexpression of GO-Y030 remains to be elucidated.

Safety of the New Curcumin Analogues

To evaluate the growth suppression of these new curcumin analogues against the normal cells, the primary human hepatocyte hNHeps was treated with new curcumin analogues. Even at concentrations as high as 100 μmol/L, GO-035 and GO-Y030 showed almost no suppression against primary hepatocytes similar to the effects observed with the most common doses of curcumin (Fig. 6A–C). For GO-Y031, growth suppression was observed to some extent at 100 μmol/L (Fig. 6D). In comparison with cancer cells, such as HCT116, these new curcumin analogues were less growth suppressive and harmless against the normal hepatocytes. Moreover, we examined the toxicity of these compounds in mice when given orally at a dose of 0.1% (w/w) daily, which dose was applied in case of curcumin (2). Judging from the body weight, behavior, and the appearance, there were no adverse effects on either mouse groups fed with GO-030 or GO-Y031 during 45 days (Fig. 6E). The longest exposure reaches at over 120 days without any changes.

Discussion

Curcumin is a dietary phytochemical that is less toxic and has an ideal potential to down-regulate the critical genes activated in cancer. However, it has some short points, including its low bioavailability claimed *in vivo*. These characters of curcumin are encouraging investigators to modify it into more aggressive forms to induce tumor suppression (23, 26, 27). Our strategy is to develop the new curcumin analogues systemically. As the results of the first screening, one direction of development, in which the 7-carbon tether of curcumin is converted to 5-carbon tether, was chosen. During the course of our work, we noted that Bowen et al. and the Shoji-Snyder team published results on the high degree of anticancer activity of diarylpentanoids, including a molecule identical to GO-035 (26, 27). However, our studies indicate that the second direction in which the location and dimensions of the substitutions on

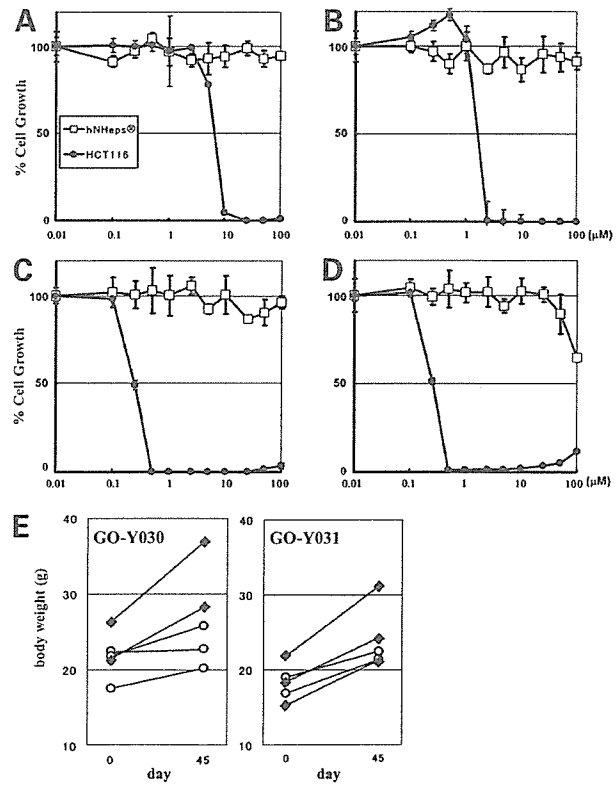

Figure 6. Safety of the new curcumin analogues. Growth-suppressive potential of curcumin analogues was evaluated against the primary hepatocyte (hNHeps; □) compared with HCT116 cells ($p53^{+/+}$; ●). **A**, curcumin. **B**, GO-035. **C**, GO-Y030. **D**, GO-Y031. **E**, safety of the new analogues (GO-Y030 and GO-Y031) *in vivo* was assessed by the body weight.

the aromatic rings are also important. The symmetrical introduction of a pair of alkoxy groups at positions 3 and 5 seems to confer considerable growth-suppressive potentials to the compounds. Several new analogues of curcumin were created in this study, some of which have shown very promising growth-suppressing properties. GO-Y030 and GO-Y031 have a higher capacity for growth suppression in many cancer cell lines than has been reported in curcumin analogues to date. Some points of success of the modification were consistent with previous reports (26, 27). It was also proposed that the unsaturated structures, such as α,β-unsaturated ketone moiety, are likely to act as Michael acceptors (26, 27); however, the effects of these structural modifications on the cellular biological reactions have not been described thus far. This is the first time that an α,β-unsaturated ketone modification has been shown to be important in cell growth regulation. The modification of curcumin to a diarylpentanoid and some types of the substitutions of a pair of alkoxy groups to the phenolic rings were the primary causes of the increase in the growth-suppressive activity of these molecules. GO-Y016, GO-Y030, and GO-Y031 were able to induce stronger growth suppression at a concentration much lower than that of 5-FU in the majority of cancer cell lines. GO-Y016, GO-Y030, and GO-Y031 could induce stronger growth suppression at a concentration lower than those of CPT-11 and CDDP in some types of cancer. Curcumin is a multifunctional compound that affects dozens of molecules, but the precise mechanism to suppress tumors is still unknown (4, 9, 10, 21) and further work is needed to identify the entire molecules that are directly affected with curcumin. We applied expression profile analysis to these new curcumin analogues as the first clue to resolve these issues. Especially, the mechanism of enhancement of the growth-suppressive effects of these new curcumin analogues must be opened at the molecular level. GO-035, GO-Y030, and GO-Y031 have a stronger potential to induce down-regulation of oncoproteins, including β-catenin, ErbB-2, c-Myc, cyclin D1, and Ki-ras, than curcumin. Inhibition of caspase-3-like activity diminishes the potentials of curcumin and its analogues to induce apoptosis, the degradation of β-catenin, and the down-regulation of Ki-ras. Therefore, the increased induction of caspase-3-like activity could account for not only the observed increase in apoptosis but also the growth suppression of cancer cells through the down-regulation of oncoproteins, such as β-catenin and Ki-ras. In the latter case, caspase-3 might cleave Ki-ras as well as β-catenin. We concluded that the enhanced caspase-3-like activity plays one of the important roles to enhance the potentials of new analogues. Up to now, in the cases of down-regulation of Ki-ras and β-catenin, it is defined that these genes affected with curcumin and its analogues are regulated posttranscriptionally through caspase-3-dependent pathway. On the other hand, G_2-M arrest was similarly observed in the presence and absence of the caspase-3/caspase-8 inhibitor. The down-regulation of ErbB-2, c-Myc, and cyclin D1 is also independent from caspase-3 pathway. Furthermore, we gave but not gained a complete understanding of the underlying mechanisms about apoptosis. For example, it has not been proven that apoptosis and the degradation of β-catenin with new analogues are mediated via the Fas receptor as previously shown with curcumin, which is located upstream of the caspase-3/caspase-8 pathway (28). Moreover, the overexpression of p53 does not contribute to apoptosis because the enhanced apoptosis induction with GO-Y030 was similarly observed in HCT116 cells ($p53^{-/-}$).

If the other critical target of curcumin could be identified, information about the interaction between the molecular surface of the target and the shape of the compound using computational analysis might be useful for designing further, even more effective, compounds. The abilities of these analogues to reduce or diminish the levels of β-catenin and Ki-ras expression that are particularly involved in the initiation or early steps of carcinogenesis suggest that they may be useful as a means of reducing the incidence of certain cancers, such as colorectal carcinogenesis. It is observed that there is no adverse reaction *in vivo* with these new compounds. Advancement of the potentials for the growth suppression and chemoprevention of these compounds could result in the improvement of the poor bioavailability of curcumin. *In vivo* evaluation of these compounds using animal models for several cancers should be done to clarify this point.

Acknowledgments

We thank Dr. B. Vogelstein for his kind gift of HCT116 cells ($p53^{+/+}$) and HCT116 cells ($p53^{-/-}$).

References

1. Surh YJ. Cancer chemoprevention with dietary phytochemicals. Nat Rev Cancer 2003;3:768–80.

2. Perkins S, Verschoyle RD, Hill K, et al. Chemopreventive efficacy and pharmacokinetics of curcumin in the min/+ mouse, a model of familial adenomatous polyposis. Cancer Epidemiol Biomarkers Prev 2002;11:535–40.

3. Huang MT, Wang ZY, Georgiadis CA, Laskin JD, Conney AH. Inhibitory effects of curcumin on tumor initiation by benzo[*a*]pyrene and 7,12-dimethylbenz[*a*]anthracene. Carcinogenesis 1992;13:2183–6.

4. Dorai T, Aggarwal BB. Role of chemopreventive agents in cancer therapy. Cancer Lett 2004;215:129–40.

5. Singh S, Aggarwal BB. Activation of transcription factor NF-κB is suppressed by curcumin (diferuloylmethane). J Biol Chem 1995;270:24995–5000.

6. Surh YJ, Han SS, Keum YS, Seo HJ, Lee SS. Inhibitory effects of curcumin and capsaicin on phorbol ester-induced activation of eukaryotic transcription factors, NF-κB and AP-1. Biofactors 2000;1:107–12.

7. Chun KS, Keum YS, Han SS, Song YS, Kim SH, Surh YJ. Curcumin inhibits phorbol ester-induced expression of cyclooxygenase-2 in mouse skin through suppression of extracellular signal-regulated kinase activity and NF-κB activation. Carcinogenesis 2003;24:1515–24.

8. Park MJ, Kim EH, Park IC, et al. Curcumin inhibits cell cycle progression of immortalized human umbilical vein endothelial (ECV304) cells by up-regulating cyclin-dependent kinase inhibitor, p21WAF1/CIP1, p27KIP1, and p53. Int J Oncol 2002;21:379–83.

9. Hong RL, Spohn WH, Hung MC. Curcumin inhibits tyrosine kinase activity of p185neu and also depletes p185neu. Clin Cancer Res 1999;5:1884–91.

10. Jaiswal AS, Marlow BP, Gupta N, Narayan S. β-Catenin-mediated transactivation and cell-cell adhesion pathways are important in curcumin (diferuylmethane)-induced growth arrest and apoptosis in colon cancer cells. Oncogene 2002;21:8414–27.

11. Kolligs FT, Nieman MT, Winer I, et al. ITF-2, a downstream target of the Wnt/TCF pathway, is activated in human cancers with β-catenin defects and promotes neoplastic transformation. Cancer Cell 2002;1: 145 – 55.

12. Rubinfeld B, Albert I, Porfiri E, Fiol C, Munemitsu S, Polakis P. Binding of GSK3β to the APC-β-catenin complex and regulation of complex assembly. Science 1996;272:1023 – 6.

13. Wong NA, Pignatelli M. β-Catenin—a linchpin in colorectal carcinogenesis? Am J Pathol 2002;160:389 – 401.

14. Shibata H, Toyama K, Shioya H, et al. Rapid colorectal adenoma formation initiated by conditional targeting of the Apc gene. Science 1997;278:120 – 3.

15. Munemitsu S, Albert I, Souza B, Rubinfeld B, Polakis P. Regulation of intracellular β-catenin levels by the adenomatous polyposis coli (APC) tumor-suppressor protein. Proc Natl Acad Sci U S A 1995;92:3046 – 50.

16. Sharma RA, Euden SA, Platton SL, et al. Phase I clinical trial of oral curcumin: biomarkers of systemic activity and compliance. Clin Cancer Res 2004;10:6847 – 54.

17. Garcea G, Berry DP, Jones DJ, et al. Consumption of the putative chemopreventive agent curcumin by cancer patients: assessment of curcumin levels in the colorectum and their pharmacodynamic consequences. Cancer Epidemiol Biomarkers Prev 2005;14:120 – 5.

18. Bunz F, Dutriaux A, Lengauer C, et al. Requirement for p53 and p21 to sustain G_2 arrest after DNA damage. Science 1998;282:1497 – 501.

19. Kakudo Y, Shibata H, Otsuka K, Kato S, Ishioka C. Lack of correlation between p53-dependent transcriptional activity and the ability to induce apoptosis among 179 mutant p53s. Cancer Res 2005;65:2108 – 14.

20. Zhou LJ, Zhu XZ. Reactive oxygen species-induced apoptosis in PC12 cells and protective effect of bilobalide. J Pharmacol Exp Ther 2000;293: 982 – 8.

21. Shim JS, Kim JH, Cho HY, et al. Irreversible inhibition of CD13/aminopeptidase N by the antiangiogenic agent curcumin. Chem Biol 2003; 10:695 – 704.

22. Baba I, Shirasawa S, Iwamoto R, et al. Involvement of deregulated epiregulin expression in tumorigenesis *in vivo* through activated Ki-Ras signaling pathway in human colon cancer cells. Cancer Res 2000;60: 6886 – 9.

23. Youssef KM, El-Sherbeny MA, El-Shafie FS, Farag HA, Al-Deeb OA, Awadalla SA. Synthesis of curcumin analogues as potential antioxidant, cancer chemopreventive agents. Arch Pharm (Weinheim) 2004;337: 42 – 54.

24. Bech-Otschir D, Kraft R, Huang X, et al. COP9 signalosome-specific phosphorylation targets p53 to degradation by the ubiquitin system. EMBO J 2001;20:1630 – 9.

25. Choudhuri T, Pal S, Agwarwal ML, Das T, Sa G. Curcumin induces apoptosis in human breast cancer cells through p53-dependent Bax induction. FEBS Lett 2002;512:334 – 40.

26. Robinson TP, Ehlers T, Hubbard IR, et al. Design, synthesis, and biological evaluation of angiogenesis inhibitors: aromatic enone and dienone analogues of curcumin. Bioorg Med Chem Lett 2003;13:115 – 7.

27. Adams BK, Ferstl EM, Davis MC, et al. Synthesis and biological evaluation of novel curcumin analogs as anti-cancer and anti-angiogenesis agents. Bioorg Med Chem 2004;12:3871 – 83.

28. Bush JA, Cheung KJ, Jr., Li G. Curcumin induces apoptosis in human melanoma cells through a Fas receptor/caspase-8 pathway independent of p53. Exp Cell Res 2001;271:305 – 14.

Human Pathology (2007) 38, 134–139

ELSEVIER

Human PATHOLOGY

www.elsevier.com/locate/humpath

Original contribution

Differential expression of ABCF2 protein among different histologic types of epithelial ovarian cancer and in clear cell adenocarcinomas of different organs☆

Sadako Nishimura MD, PhD[a], Hiroshi Tsuda MD, PhD[a,f,*], Kiyoshi Ito MD, PhD[b], Toshiko Jobo MD, PhD[c], Nobuo Yaegashi MD, PhD[b], Takeshi Inoue MD, PhD[d], Tamotsu Sudo MD, PhD[e], Ross S. Berkowitz MD[f], Samuel C. Mok PhD[f]

[a]*Department of Obstetrics and Gynecology, Osaka City General Hospital, Miyakojima, Osaka 534-0021, Japan*
[b]*Department of Obstetrics and Gynecology, Tohoku University Graduate School of Medicine, Sendai 980-8574, Japan*
[c]*Department of Obstetrics and Gynecology, School of Medicine Kitasato University, Sagamihara 228-8555, Japan*
[d]*Department of Pathology, Osaka City General Hospital, Miyakojima, Osaka 534-0021, Japan*
[e]*Department of Clinical Research, Hyogo Medical Center for Adults, Akashi 673-8558, Japan*
[f]*Department of Obstetrics, Gynecology and Reproductive Biology, Laboratory of Gynecologic Oncology, Brigham and Women's Hospital, Harvard Medical School, Boston, MA 02115, USA*

Received 3 May 2006; revised 17 June 2006; accepted 21 June 2006

Keywords:
ABC transporter;
Clear cell adenocarcinoma;
Kidney;
Endometrium

Summary Previously, we reported that ABCF2 protein expression is higher in clear cell than serous histotype of ovarian adenocarcinomas and that its expression correlates with chemoresponse in patients with clear cell ovarian cancer. In this study, we examined ABCF2 protein expression in mucinous, endometrioid, and poorly differentiated type of ovarian adenocarcinomas. In addition, ABCF2 expression was evaluated in clear cell adenocarcinomas derived from different organs. A total of 335 epithelial ovarian cancers, 23 clear cell adenocarcinomas of uterine corpus, and 34 clear cell adenocarcinomas of kidney were included in this study. ABCF2 protein expression was determined by immunohistochemistry. The results showed that cytoplasmic ABCF2 expression was significantly higher in clear cell–type ovarian cancer specimens compared with other types ($P < .0001$). There was a close relationship between nuclear ABCF2 expression levels and age of patients with clear cell ovarian cancer. Multivariate logistic regression model also demonstrated that cytoplasmic ABCF2 expression was associated with clear cell histology (odds ratio, 5.557; 95% confidence interval, 2.694-11.462; $P < .0001$). In addition, both clear cell adenocarcinomas of the ovary and the uterine corpus showed significantly higher levels of ABCF2 expression, compared with those of the clear cell adenocarcinoma

☆ This study was supported in part by a Grant from Osaka City General Hospital (Osaka, Japan), Dana-Farber/Harvard Cancer Center (Boston, MA) Ovarian Cancer SPORE Grant P50CA165009, and Grant R33CA103595 from National Institutes of Health, Department of Health and Human Services (Bethesda, MD) and Gillette Center For Women's Cancer (Boston, MA).

* Corresponding author. Department of Obstetrics and Gynecology, Osaka City General Hospital, Miyakojima, Osaka 534-0021, Japan.
E-mail address: htsud@s5.dion.ne.jp (H. Tsuda).

doi:10.1016/j.humpath.2006.06.026

of the kidney ($P < .0001$). These data suggest that ABCF2 protein may be a candidate marker for clear cell adenocarcinomas of the ovary and the uterine corpus and may be important for the pathogenesis of these diseases.

1. Introduction

Resistance to chemotherapeutic agents is a major obstacle for successful treatment of cancer. The sensitivity to chemotherapy is generally related to pathologic findings, such as histologic type or grade of the tumor, even if they share the same origin. For example, epithelial ovarian cancer can be subdivided into 5 major histologic types (serous, mucinous, endometrioid, clear cell, and poorly differentiated). Among them, clear cell ovarian cancer, which constitutes 5% to 10% of ovarian cancer cases in the Unites States, differs from other histologic types with respect to its clinical characteristics [1,2]. Clear cell ovarian cancer is usually more resistant to systemic chemotherapy than other types and has a worse prognosis [3,4]. We previously reported that ABCF2 protein expression is higher in clear cell type than serous type, and its expression correlates with chemoresponse in patients with clear cell ovarian cancer [5]. In this study, we further examined ABCF2 protein expression in mucinous, endometrioid, and poorly differentiated types of ovarian cancer and compared it with that of the clear cell and serous types.

Clear cell adenocarcinomas have been found to develop in different organs such as the ovary, the uterine corpus, and the kidney, and the prognosis of this cancer is usually poor [3,4,6,7]. In the cancer of uterine corpus, clear cell and serous adenocarcinomas have worse prognosis, compared with that of the endometrioid type, which constitutes 80% of uterine corpus cancer [6]. Clear cell adenocarcinoma of the kidney is thought to be chemoresistant [7,8]. Clear cell adenocarcinoma of the ovary is morphologically similar to clear cell adenocarcinomas developed from the uterine corpus or the kidney. However, both clear cell adenocarcinomas of the ovary and uterine corpus are Mullerian in origin, whereas those developed from the kidney are Wolffian duct in origin [9]. Candidate biomarkers that can be used successfully to differentiate these tumors have not been identified. In this study, we further evaluated whether significant differences in ABCF2 protein expression can be identified in clear cell adenocarcinoma of the ovary, the uterine corpus, and the kidney.

2. Materials and methods

2.1. Clinical samples

A total of 335 epithelial ovarian cancers, 23 clear cell adenocarcinomas of uterine corpus, and 34 clear cell adenocarcinomas of kidney were included in this study. Median age of patients with ovarian cancer is 54 years (range, 22-85 years). In ovarian cancer, histologic types were as follows: 102 serous adenocarcinomas, 50 mucinous adenocarcinomas, 76 clear cell adenocarcinomas, 74 endometrioid adenocarcinomas, and 33 undifferentiated carcinomas. Twenty-two of 76 clear cell cases and 15 of 102 serous cases were previously reported [5]. Median age of patients with clear cell adenocarcinoma of the uterine corpus and the kidney is 62 (range, 48-83) and 65 (range, 30-86) years. The clinical background is shown in Table 1. All patient-derived paraffin sections were collected and archived under protocols approved by the institutional review boards of the parent institutions.

2.2. Immunohistochemistry

Immunolocalization of the ABCF2 protein was performed using a polyclonal anti-ABCF2 antibody generated by injecting the purified full-length ABCF2 fusion protein into

Table 1 Clinical background of each histologic type

	Clinical stage		Histologic grade		
	Stage I + II	Stage III + IV	Well/moderate	Poor	Total
Epithelial ovarian cancer					
Serous	34	68	70	32	102
Mucinous	34	16	48	2	50
Clear cell	47	29	65	11	76
Endometrioid	30	44	44	30	74
Poorly differentiated	4	29	0	33	33
Total					336
Clear cell adenocarcinoma					
Uterine corpus	14	9	–	–	23
Kidney	24	10	–	–	34

Table 2 ABCF2 expression in epithelial ovarian cancer

Parameter	ABCF2 (cytoplasm)			ABCF2 (nuclear)	
	Positive	Negative	*P*	LI (95% CI)	*P*
Age					
<Median	104	64	NS	7.1 (4.9-9.3)	.004
>Median	106	62		13.7 (9.8-17.5)	
FIGO stage					
I + II	100	49	NS	12.2 (8.8-15.5)	NS
III + IV	110	77		9.1 (6.1-12.1)	
Histologic type					
Clear	66	10		21.1 (15.5-26.8)	
Serous	54	48	<.0001	10.2 (5.8-14.6)	.01
Mucinous	23	27	<.0001	4.2 (1.8-6.6)	.0003
Endometrioid	43	31	<.0001	4.7 (1.8-7.6)	<.0001
Undifferentiated	24	10	NS	9.1 (0.04-18.1)	.03
Differentiation grade					
Well/moderate	141	86	NS	11.2 (8.6-13.8)	NS
Poor	69	40		8.8 (4.6-13.1)	

Abbreviations: LI, labeling index; NS, nonsignificant; FIGO, International Federation of Gynecologists and Obstetricians.

the rabbits [5]. In brief, histologic sections (4 μm) were affixed to glass slides, dewaxed, and rehydrated. The sections were then incubated in 3% hydrogen peroxide for 10 minutes at room temperature to quench endogeneous peroxidase activity. The sections were reacted with the ABCF2 antibody (×5000) at 4°C overnight. The peroxidase activity for all proteins was visualized by applying diaminobenzidine chromogen containing 0.05% hydrogen peroxide for 2 to 10 minutes at room temperature. The sections were then counterstained with hematoxylin. The slides were read by 2 independent pathologists who were blinded to the clinical background of the patients. Positive cells were counted for ABCF2 protein in the nuclei by examining at least 1000 tumor cells. Levels of ABCF2 were scored based on the percentage of cells with positive nuclear staining. ABCF2 cytoplasmic staining groups were divided into positive or negative. Slides of epithelial ovarian cancer known to be either positive or negative for ABCF2 expression were used as positive and negative controls, respectively [5].

2.3. Statistical analysis

The relationship between ABCF2 expression and age, clinical stage, and histologic grade were analyzed using *t* test and χ^2 test. Differences of ABCF2 expression in cytoplasm among the histologic groups of ovarian cancer were analyzed by the method of Ryan [10]. Differences of ABCF2 expression in nuclei among the histologic groups of ovarian cancer were examined by 1-way analysis of variance, followed by Tukey-Kramer tests. To determine whether any significant effects could be explained by other variables, a multivariate logistic regression model or multivariate regression model was performed with the following covariates in the model: age in years, clinical stage, histologic type, and histologic grade.

The comparison of ABCF2 expression in nuclei and cytoplasm in clear cell adenocarcinoma of ovary, endometrium, and kidney were evaluated using *t* test and χ^2 test.

3. Results

3.1. ABCF2 expression in ovarian cancer

In all histologic types of ovarian cancer, nuclear ABCF2 expression was lower in the younger age group (less than median age) (7.1 versus 13.7, $P = .004$) (Table 2). However, there was no significant difference in ABCF2 in cytoplasm expression between both groups. There was no significant relationship between clinical stage, histologic grade, and

Fig. 1 A, Positive immunostaining of ABCF2 in clear cell adenocarcinoma of the ovary. B, Negative immunostaining of ABCF2 in clear cell adenocarcinoma of the ovary. C, Positive immunostaining of ABCF2 in serous cystadenocarcinoma. D, Negative immunostaining of ABCF2 in serous cystadenocarcinoma. E, Positive immunostaining of ABCF2 in mucinous cystadenocarcinoma. F, Negative immunostaining of ABCF2 in mucinous cystadenocarcinoma. G, Positive immunostaining of ABCF2 in endometrioid adenocarcinoma. H, Negative immunostaining of ABCF2 in endometrioid adenocarcinoma. I, Positive immunostaining of ABCF2 in undifferentiated adenocarcinoma. J, Negative immunostaining of ABCF2 in undifferentiated adenocarcinoma. K, Immunostaining of ABCF2 in normal ovary. L, Positive immunostaining of ABCF2 in clear cell adenocarcinoma of the uterine corpus. M, Negative immunostaining of ABCF2 in clear cell adenocarcinoma of the uterine corpus. N, Positive immunostaining of ABCF2 in clear cell adenocarcinoma of the kidney. O, Negative immunostaining of ABCF2 in clear cell adenocarcinoma of the kidney.

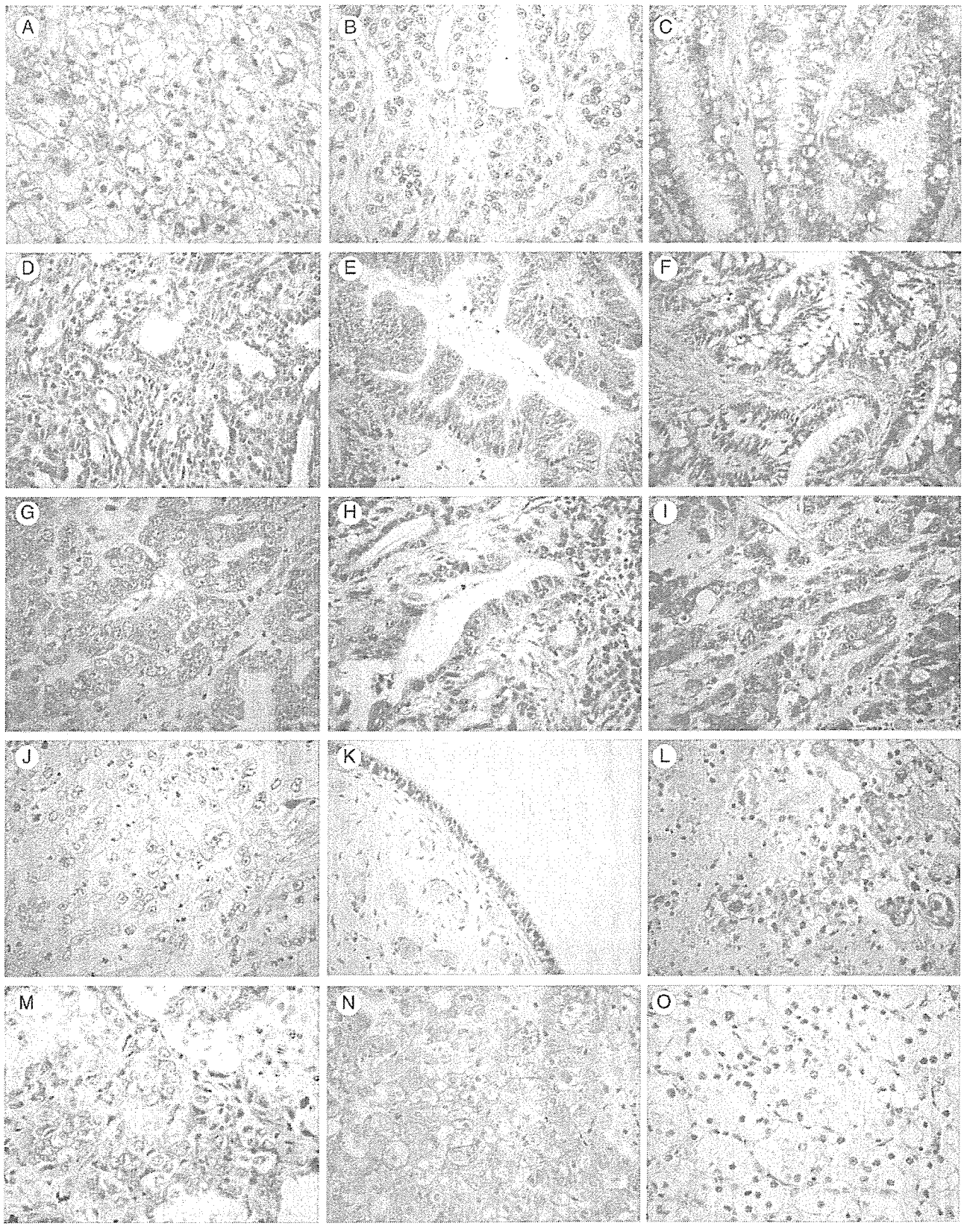
A
B
C
D
E
F
G
H
I
J
K
L
M
N
O

Table 3 Multivariable predictors of ABCF2 expression

Parameter	ABCF2 (cytoplasm)			ABCF2 (nuclear)		
	OR	95% CI	*P*	OR	95% CI	*P*
Age	1.119	0.699-1.791	.639	7.254	2.953-11.556	.001
FIGO stage	0.778	0.477-1.27	.316	−2.035	−6.485 to 2.414	.369
Histologic type	5.557	2.694-11.462	<.0001	13.587	8.345-18.829	<.001
Histologic grade	0.692	0.416-1.152	.157	0.375	−4.388-5.087	.876

NOTE. Age, greater than versus less than median; Stage, III + IV versus I + II; Histologic type, clear cell versus non–clear cell; histologic grade, well/moderate versus poor.

ABCF2 expression in nuclei or cytoplasm (Table 2). Labeling index of ABCF2 expression in nuclei is higher in clear cell adenocarcinoma than in serous, mucinous, endometrioid, and undifferentiated adenocarcinoma (21.1 versus 10.2, 4.2, 4.7, and 9.1; P = .01, .0003, <.0001, and .03, respectively) (Table 2). The frequency of ABCF2 expression in cytoplasm was 86.8%, 52.9%, 46.0%, 58.1%, and 70.6% in clear cell, serous, mucinous, endometrioid, and undifferentiated types, and it is higher in clear cell than in serous, mucinous, and endometrioid adenocarcinoma (P < .0001) (Table 2). Representative images of immunolocalization of ABCF2 in ovarian cancer and normal ovary are shown in Fig. 1A-K. Normal ovarian epithelium was weakly stained.

The multivariate logistic regression model showed that clear cell histology was associated with ABCF2 expression in cytoplasm (odds ratio [OR], 5.557; 95% confidence interval [CI], 2.694-11.462; P < .0001). The multivariate regression model showed that age greater than median age and clear cell histology were associated with ABCF2 expression in nuclei (OR, 7.254; 95% CI, 2.953-11.556; P = .001) (OR, 13.587; 95% CI, 8.345-18.829; P < .001) (Table 3).

3.2. ABCF2 expression in clear cell adenocarcinoma of the ovary, uterine corpus, and the kidney

There were no significant differences in ABCF2 nuclear or cytoplasmic expression between clear cell adenocarcinoma of the ovary and the uterine corpus. However, the cytoplasmic and nuclear ABCF2 expression rate was significantly higher in clear cell adenocarcinoma of the ovary and uterine corpus than in the kidney (86.8% versus 38.2%, P < .0001; 21.1 versus 1.9, P < .0001) (Table 4). ABCF2 expression was not associated with clinical stage in clear cell adenocarcinoma of the ovary, the uterine corpus, and the kidney. Representative images of immunohistochemistry of clear cell adenocarcinoma of uterine corpus and kidney are shown in Fig. 1L-O.

4. Discussion

Clear cell ovarian cancer is a relatively uncommon histologic type of epithelial ovarian cancer, and its molecular basis remains unclear. We previously reported that ABCF2 protein is highly expressed in clear cell type compared with serous-type ovarian cancer, and its expression is related to chemotherapy response [5]. In this study, we further investigate ABCF2 protein expression patterns among 5 histologic types of epithelial ovarian cancer. The results showed that clear cell cancer expressed significantly higher levels of ABCF2 than that of other histologic types. It is particularly interesting that clear cell and endometrioid type of ovarian cancers expressed different levels of ABCF2 in spite that both of them are believed to develop from endometriosis [2]. These findings further support the hypothesis that different histologic types of ovarian cancer have different pathogenetic pathways, and ABCF2 may play different roles in different histologic types of ovarian cancer.

In this study, we found that ABCF2 was expressed in 86.8% of clear cell ovarian cancer. In addition, we showed that ABCF2 was expressed in 89.4% of stage I and II clear cell cancers. These data suggest that ABCF2 may be used as a marker for early detection of the disease. Currently, CA125, a glycoprotein recognized by the monoclonal antibody OC125 [11], is found to be elevated in more than 80% of ovarian cancer, and it is an excellent tumor marker of ovarian cancer [12]. However, CA125 elevation rate is relatively low in clear cell ovarian cancer or in early stage of ovarian cancer [13,14]. Because clear cell type of ovarian cancer is usually more resistant to systemic chemotherapy than other histologic types and has a worse prognosis [3,4], early diagnosis is essential especially for clear cell ovarian cancer. Finding new tumor markers for this type of ovarian tumor is particularly important.

Clear cell adenocarcinoma can arise from the ovary, the uterine corpus, and the kidney. These 3 types of clear cell adenocarcinomas are morphologically indistinguishable from one another. It has been shown that clear cell adenocarcinomas of both ovary and kidney are chemoresistant [3,4,7,8]. Molecular markers that can be used to differentiate clear cell cancers in different organs have not been identified. In addition, the mechanism of chemoresistance of kidney clear cell adenocarcinoma may differ from that in clear cell adenocarcinoma of ovary or uterine corpus. The differential expression patterns may be explained by the fact that both clear cell adenocarcinoma of the ovary and uterine corpus are Mullerian in origin, in

Table 4 ABCF2 expression in clear cell adenocarcinoma of each site

	Cytoplasmic staining	*P*	Nuclear staining	*P*
Ovary	86.8% (66/76)		21.1	
Uterine corpus	91.3% (21/23)	ns	11.5	ns
Kidney	38.2% (13/34)	<.0001	1.9	<.0001

contrast to clear cell adenocarcinoma of the kidney, which is Wolffian duct in origin [8].

In conclusion, our findings suggest that ABCF2 protein may be used as a biomarker to detect clear cell ovarian cancer at early stages and may be important for the pathogenesis of clear cell cancers of Mullerian origin.

Acknowledgment

The authors thank Dr Naoki Kawamura of Osaka City General Hospital for his critical review of the manuscript and Asami Nagata and Nozomi Tsuji for their technical assistance.

References

[1] Scully RE, Young RH, Clement PB. Tumors of the ovary, maldeveloped gonads, fallopian tube, and broad ligament. Atlas of Tumor Pathology. 3rd series, Fascicle 23. Washington (DC): Armed Forces Institute of Pathology; 1998.

[2] Russel P. Surface epithelial-stroma tumors of the ovary. In: Kurman RJ, editor. Blaustein's pathology of the female genital tract. 4th ed. New York: Springer-Verlag; 1994. p. 705-82.

[3] Goff BA, Sainz de la Cuesta R, Muntz HG, et al. Clear cell carcinoma of the ovary: a distinct histologic type with poor prognosis and resistance to platinum-based chemotherapy in stage 3 disease. Gynecol Oncol 1996;60:412-7.

[4] Behbakht K, Randall TC, Benjamin I, Morgan MA, King S, Rubin SC. Clinical characteristics of clear cell carcinoma of the ovary. Gynecol Oncol 1998;70:255-8.

[5] Tsuda H, Ito YM, Ohashi Y, et al. Identification of overexpression and amplification of ABCF2 in clear cell ovarian adenocarcinomas by cDNA microarray analyses. Clin Cancer Res 2005;11:6880-8.

[6] Abeler VM, Kjorstad KE, Berle E. Carcinoma of the endometrium in Norway: a histopathological and prognostic survey of a total population. Int J Gynecol Cancer 1992;2:9-22.

[7] Yagoda A. Phase II cytotoxic chemotherapy trials in RCC: 1983-1988. Prog Clin Biol Res 1990;350:227-41.

[8] Bukowski RM. Natural history and therapy of metastatic renal cell carcinoma. Cancer 1997;80:1198-220.

[9] Matias-Guiu X, Lerma E, Part J. Clear cell tumors of the female genital tract. Semin Diagn Pathol 1997;14:233.

[10] Ryan TA. Significance tests for multiple comparison of proportions, variances, and other statistics. Psychol Bull 1960;57:318-28.

[11] Bast RC, Feeney M, Lazarus H, Nadler LM, Colvin RB, Knapp RC. Reactivity of a monoclonal antibody with human ovarian carcinoma. J Clin Invest 1981;68:1331-7.

[12] Bast Jr RC, Klug TL, St John E, et al. A radioimmunoassay using a monoclonal antibody to monitor the course of epithelial ovarian cancer. N Engl J Med 1983;309:883-7.

[13] Jacobs I, Bast Jr RC. The CA125 tumour-associated antigen: a review of the literature. Hum Reprod 1989;4:1-12.

[14] Vergote IB, Bormer OP, Abeler VM. Evaluation of serum CA125 levels in the monitoring of ovarian cancer. Am J Obstet Gynecol 1987;157:88-92.

Int J Gynecol Cancer 2006, **16**, 979–985

ORIGINAL ARTICLES

Genetic variation in *ABCB1* influences paclitaxel pharmacokinetics in Japanese patients with ovarian cancer

H. YAMAGUCHI*†, T. HISHINUMA*†, N. ENDO*, H. TSUKAMOTO*, Y. KISHIKAWA†, M. SATO†, Y. MURAI†, M. HIRATSUKA‡, K. ITO§, C. OKAMURA§, N. YAEGASHI§, N. SUZUKI*†, Y. TOMIOKA*† & J. GOTO*†

**Division of Clinical Pharmacy, Graduate School of Pharmaceutical Sciences, Tohoku University, Sendai, Japan; †Department of Pharmaceutical Sciences, Tohoku University Hospital, Sendai, Japan; ‡Department of Clinical Pharmaceutics, Tohoku Pharmaceutical University, Sendai, Japan; and §Department of Obstetrics and Gynecology, Graduate School of Medicine, Tohoku University, Sendai, Japan*

Abstract. Yamaguchi H, Hishinuma T, Endo N, Tsukamoto H, Kishikawa Y, Sato M, Murai Y, Hiratsuka M, Ito K, Okamura C, Yaegashi N, Suzuki N, Tomioka Y, Goto J. Genetic variation in *ABCB1* influences paclitaxel pharmacokinetics in Japanese patients with ovarian cancer. *Int J Gynecol Cancer* 2006;**16**:979–985.

Paclitaxel, an antineoplastic agent used for the treatment of ovarian cancer, is metabolized by cytochrome P450 (CYP)3A4 and CYP2C8 and is excreted from cells by ATP-binding cassette (ABCB1) (multi-drug resistance [MDR1], P-glycoprotein). Expression of these proteins is regulated by pregnane X receptor (PXR). Although there are common genetic polymorphisms in the genes encoding these proteins, their effect on the clinical efficacy of paclitaxel is unclear. We therefore examined the relationship of the paclitaxel pharmacokinetics in 13 patients with ovarian cancer to polymorphisms in *CYP2C8*, *CYP3A5*, *ABCB1*, and *PXR*. We found high interindividual variability in the plasma concentrations of two metabolites, 6α-hydroxypaclitaxel and *p*-3′-hydroxypaclitaxel. All the patients were genotyped as *CYP2C8*1/*1*. Neither the *CYP3A5* A6986G (*CYP3A5*3*) nor the *PXR* C-25385T alleles were associated with altered plasma concentrations of paclitaxel and its metabolites. *ABCB1* T-129C, T1236C, and G2677(A,T), however, was associated with lower area under the plasma concentration–time curve (AUC) of paclitaxel. We also observed a significant correlation between the AUC ($r = -0.721$) or the total clearance of paclitaxel (CL_{tot}) ($r = 0.673$) and the *ABCB1* mutant allele dosage in each patient. Taken together, our findings suggest that interindividual variability in paclitaxel pharmacokinetics could be predicted by *ABCB1* genotyping.

KEYWORDS: ABCB1, genetic polymorphisms, ovarian cancer, paclitaxel pharmacokinetics.

Paclitaxel has a significant clinical activity against multiple cancers, including ovarian, breast, and lung tumors[1]. The stabilization of microtubules by paclitaxel results in cell cycle arrest. Although highly effective, earlier studies have demonstrated a high degree of interindividual variability in resulting plasma paclitaxel concentrations[2]. Paclitaxel therapy is typically associated with a number of toxic side effects, most commonly neutropenia, peripheral neuropathy, nausea, and vomiting[3]. Previous studies reported a correlation between toxicity and paclitaxel plasma

Address correspondence and reprint requests to: Junichi Goto, PhD, Department of Pharmaceutical Sciences, Tohoku University Hospital, 1-1 Seiryo-machi, Aoba-ku, Sendai 980-8574, Japan. Email: jun-goto@pharm.med.tohoku.ac.jp

H. Tsukamoto is presently at Institute for Environmental and Gender Specific Medicine, Graduate School of Medicine, Juntendo University, Urayasu, Japan; and N. Suzuki is presently at Department of Clinical Pharmacy, Faculty of Pharmaceutical Sciences, Josai International University, Togane, Japan.

concentrations when the drug was given at lower doses or during shorter infusion times[4,5]. The mechanisms underlying the interindividual variabilities of drug toxicity, however, remain poorly understood.

Systemic elimination of paclitaxel occurs primarily via hepatic metabolism and biliary excretion[6]. Formation of the major metabolite, 6α-hydroxypaclitaxel, is catalyzed by cytochrome P450 (CYP) 2C8[7,8], while the other metabolite, *p*-3′-hydroxypaclitaxel, is formed by the action of CYP3A4[7,9]. The dihydroxylated metabolite is thought to result from the stepwise hydroxylation of the two previously described sites. Although CYP3A5 is not responsible for paclitaxel hydroxylation[9], Kuehl *et al.*[10] reported that this protein can account for greater than 50% of the total CYP3A in people who express this allele. Therefore, CYP3A5 polymorphisms may contribute to the observed interindividual differences in paclitaxel clearance. Paclitaxel is also a substrate of the drug efflux transporter ABCB1 (MDR1, P-glycoprotein)[11,12], which is normally expressed in the billiary tract, intestine, renal tubules, and brain. ABCB1 plays a principal role in maintenance of the absorption barrier and elimination of xenobiotics, such as paclitaxel, from the body[13]. The pregnane X receptor (PXR) is a xenobiotic-regulated transcription factor that coordinately activates transcription of *CYP2C8* and *CYP3A4* in the liver and *ABCB1* in the intestine[14]. Thus, PXR is a master regulator of drug clearance; any functional variants will likely have widespread effects on paclitaxel pharmacokinetics. Although common genetic polymorphisms in these genes could influence paclitaxel efficacy, the relationship of these alleles to paclitaxel pharmacokinetics has not been fully evaluated.

In this study, we examined the pharmacokinetics of paclitaxel and metabolites formed by CYP2C8 or CYP3A4 and known functional polymorphisms of *CYP2C8*, *CYP3A5*, *ABCB1*, and *PXR*. In Japanese patients undergoing paclitaxel and carboplatin combination therapy for diagnosed ovarian cancer, we then correlated these genotypes with paclitaxel pharmacokinetics.

Materials and methods

Patients

Paclitaxel pharmacokinetics was studied in 13 patients with newly diagnosed ovarian cancer undergoing first-line chemotherapy. The mean age of the patients was 53 years, ranging from 31 to 73 years (Table 1). All clinical protocols, including blood sampling for pharmacokinetic and pharmacogenetic analyses, were approved by the ethical committee of Tohoku University School of Medicine. Genotyping was performed in above-mentioned patients and unrelated healthy Japanese volunteers. All subjects provided their written informed consent for participation in the sampling protocol.

Table 1. Patient characteristics

Characteristic	Patients
Age, mean ± SD (years)	53 ± 12
Body surface area, mean ± SD (m^2)	1.45 ± 0.09
Sampling time points after paclitaxel infusion	
1, 3, 6, and 19 h	3
3, 6, 9, and 19 h	1
3, 4, 6, 9, and 19 h	3
1, 2, 3, 4, 6, 9, and 19 h	6

Genotyping

Genomic DNA was extracted from peripheral blood cells, treated with K_2EDTA as an anticoagulant, using a GFX Genomic Blood DNA Purification Kit (Amersham Pharmacia Biotech, Buckinghamshire, UK), according to the manufacturer's recommendations. *CYP2C8* A805T (*CYP2C8*2*), G416A/A1196G (*CYP2C8*3*), and C792G (*CYP2C8*4*), and *ABCB1* T-129C, T1236C, G2677(A,T), and C3435T were genotyped by polymerase chain reaction (PCR)–restriction enzyme fragment length polymorphism as previously described with minor modification[15–17]. The *CYP2C8* 475A deletion (*CYP2C8*5*) and the C1210G, *CYP3A5* A6986G (*CYP3A5*3*), and *PXR* C-25385T alleles were genotyped by allele-specific real-time PCR with SYBR Green using an ABI PRISM 7700 sequence detection system (Applied Biosystems, Foster City, CA) as described[18]. Briefly, in a 20 μL reaction mixture containing 2× SYBR Green PCR Master Mix (QIAGEN, Valencia, CA), 0.4 μM forward and reverse primers were used to amplify the specified sequences from 20 to 100 ng genomic DNA. PCR products were detected following amplification by 1 cycle of 95°C for 15 min and 35 cycles of 95°C for 30 sec, 60°C for 30 sec, and 72°C for 30 sec. The PCR primers used are shown in Table 2.

Pharmacokinetics studies

Paclitaxel was administered intravenously over a 3-h infusion period at a dose of approximately 175 mg/m^2 (163–194 mg/m^2). Plasma samples were obtained at four to seven time points within 1–19 h after the start of the infusion. After centrifugation, plasma samples were stored at –80°C until analysis. We measured the concentrations of paclitaxel, 6α-hydroxypaclitaxel, and

Table 2. Summary of primer pair sequences (5′–3′) used in allele-specific real-time PCR assays with SYBR Green

CYP2C8	
475A deletion	
(*CYP2C8*5*)	
WP	GTCACCCACCCTTGGTTTTTC
MP	GTCACCCACCCTTGGTTTTC
CP	TGAATTCTCCCAGTTTCTGCCC
C1210G	
WP	GCTACATGATGACAAAGAATTTCCTAATC
MP	GCTACATGATGACAAAGAATTTCCTAATG
CP	CCTTTAAATACAAATGGAAACGAG
CYP3A5	
A6986G	
(*CYP3A5*3*)	
WP	TCTCTTTAAAGAGCTCTTTTGTCTTTCGA
MP	TCTCTTTAAAGAGCTCTTTTGTCTTTCGG
CP	CAACCTTAGGTTCTAGTTCATTAGGGTG
PXR	
C-25385T	
WP	CATTTTTTGGCAATCCCAGGTTC
MP	CATTTTTTGGCAATCCCAGGTTT
CP	AGATGCTTTATGGCAGGTGAGGG

WP, wild-type primer; MP, mutant primer; CP, common primer.

p-3′-hydroxypaclitaxel in all patients by reverse-phase high-performance liquid chromatography as described[19]. Briefly, cephalomannine was added to each plasma sample as an internal standard. Paclitaxel, 6α-hydroxypaclitaxel, and *p*-3′-hydroxypaclitaxel were extracted using a 1-mL Bond Elut C18 cartridge (Varian, Harbor City, CA). The high-performance liquid chromatography system consisted of a Nanospace SI-1 (Shiseido, Tokyo, Japan) equipped with an ultraviolet ray detector at 230 nm. Chromatography was performed on a C18 Capcell Pak UG120 column (Shiseido; 1.5 × 150 mm, 5 μm) at 40°C using isocratic elution in acetonitrile–20 mM ammonium acetate (38:62, vol/vol, pH 5.0) at a flow rate of 100 μL/min. The pharmacokinetic parameters, including the area under the plasma concentration–time curve (AUC), mean residence time, volume of distribution at steady state (V_{dss}), and total clearance (CL_{tot}), were calculated by moment analysis as described[20].

Statistical analysis

All pharmacokinetic data are presented as mean ± SD. To relate the pharmacokinetic parameters to each polymorphism, the Mann–Whitney *U* test was used for two group comparisons. When more than two groups were compared, the Kruskal–Wallis test was used. The correlation between the pharmacokinetic parameters and the number of *ABCB1* mutant alleles in our subjects was estimated by the Spearman rank correlation. P values < 0.05 were considered to be significant.

Results

Genotyping

There is little information concerning the frequency of *CYP2C8* and *PXR* polymorphisms in the Japanese population. In a preliminary study, we screened for previously described polymorphisms of *CYP2C8* and *PXR* in DNA samples from 210 and 90 Japanese individuals, respectively. We found only one subject genotyped as a heterozygote of *CYP2C8*3*, giving an allele frequency of 0.0024. No other polymorphisms in the *CYP2C8* gene were observed. The genotype frequencies of *PXR* were 0.511 for wild type, 0.456 for the C-25385T heterozygote, and 0.033 for homozygous C-25385T mutants. Therefore, the mutant allele frequency was 0.261, which is lower

Table 3. *CYP2C8, CYP3A5, ABCB1,* and *PXR* genotypes in 13 patients[a]

		CYP3A5	*ABCB1*				*PXR*
Patient number	*CYP2C8*	A6986G	T-129C	T1236C	G2677 (A,T)	C3435T	C-25385T
1	*1/*1	A/G	T/T	T/T	G/T	C/T	C/C
2	*1/*1	A/G	T/T	T/C	A/T	C/C	C/C
3	*1/*1	G/G	T/T	T/C	G/G	C/T	C/C
4	*1/*1	A/G	T/T	T/T	T/T	T/T	C/T
5	*1/*1	A/A	T/T	T/T	G/T	C/T	T/T
6	*1/*1	A/G	T/T	T/T	G/G	C/C	C/C
7	*1/*1	G/G	T/T	T/C	G/G	C/C	C/C
8	*1/*1	G/G	T/T	T/T	G/T	C/T	C/T
9	*1/*1	A/G	T/T	T/T	G/T	C/T	C/C
10	*1/*1	G/G	T/T	T/T	G/T	C/T	C/C
11	*1/*1	A/G	T/T	T/C	G/T	C/C	C/T
12	*1/*1	G/G	T/C	C/C	A/A	C/C	C/T
13	*1/*1	G/G	T/T	T/C	G/T	C/T	C/C

[a]The most common (wild-type) *CYP2C8* allele was *CYP2C8*1*.

than the frequencies of 0.39 and 0.32 observed for Caucasian and African American populations, respectively[21]. These results correlated well with the expected genotype distributions of the examined genes calculated by the Hardy–Weinberg equation.

We also examined the *CYP2C8*, *CYP3A5*, *ABCB1*, and *PXR* genotypes in 13 Japanese patients (Table 3). None of the 13 patients genotyped possessed the *CYP2C8*2*, *CYP2C8*3*, *CYP2C8*4*, *CYP2C8*5*, or C1210G alleles; all were genotyped as *CYP2C8*1/*1*.

Pharmacokinetics of paclitaxel

Plasma concentration–time curves of paclitaxel, 6α-hydroxypaclitaxel, and *p*-3′-hydroxypaclitaxel are shown in Figure 1; the pharmacokinetic parameters are summarized in Table 4. Interindividual variabilities between the lowest and the highest values diverged to 3.4-, 2.6-, 2.1-, and 2.3-fold for paclitaxel maximum drug concentration (C_{max}), AUC, V_{dss}, and CL_{tot}, respectively. The AUC ratios were also highly variable, with 12.5-, 5-, and 8-fold differences between the lowest and the highest values for 6α-hydroxypaclitaxel/paclitaxel (×100), *p*-3′-hydroxypaclitaxel/paclitaxel (×100), and 6α-hydroxypaclitaxel/*p*-3′-hydroxypaclitaxel, respectively. The AUC ratio of 6α-hydroxypaclitaxel to *p*-3′-hydroxypaclitaxel in patients 4, 10, and 11 was approximately 1, while this value in the remaining patients was below 1. These results suggest that the metabolic activity of CYP2C8 is similar to or slightly lower than that of CYP3A4 against paclitaxel in Japanese subjects.

Correlation of genotype and pharmacokinetic parameters

As none of the examined patients possessed *CYP2C8* variant alleles, we could not examine the correlation between paclitaxel pharmacokinetic parameters and *CYP2C8* polymorphisms.

For the *CYP3A5*1/*1*, **1/*3*, and **3/*3* genotypes (n = 1, 6, and 6), mean paclitaxel AUC were 12.0, 9.78 ± 1.43, and 10.5 ± 3.41 μg·h/mL and the *p*-3′-hydroxypaclitaxel/paclitaxel (×100) AUC ratios were 6.06, 5.21 ± 3.37, and 6.39 ± 3.20, respectively. There were no obvious trends in either the mean paclitaxel AUC or the *p*-3′-hydroxypaclitaxel/paclitaxel AUC ratio that would suggest an effect of *CYP3A5*3* genotype on these parameters.

The patient heterozygous for the *ABCB1* T-129C allele exhibited a lower paclitaxel AUC than the wild-type homozygotes (5.73 versus 10.7 ± 2.14 μg·h/mL; n = 1 versus 12). Although the differences were not statistically significant, *ABCB1* T1236C tended to be associated with lower paclitaxel AUC (11.4 ± 2.32, 9.62 ± 1.48, and 5.73 μg·h/mL for 1236T/T, T/C, and C/C genotypes [n = 7, 5, and 1], respectively). Individuals homozygous for the *ABCB1*

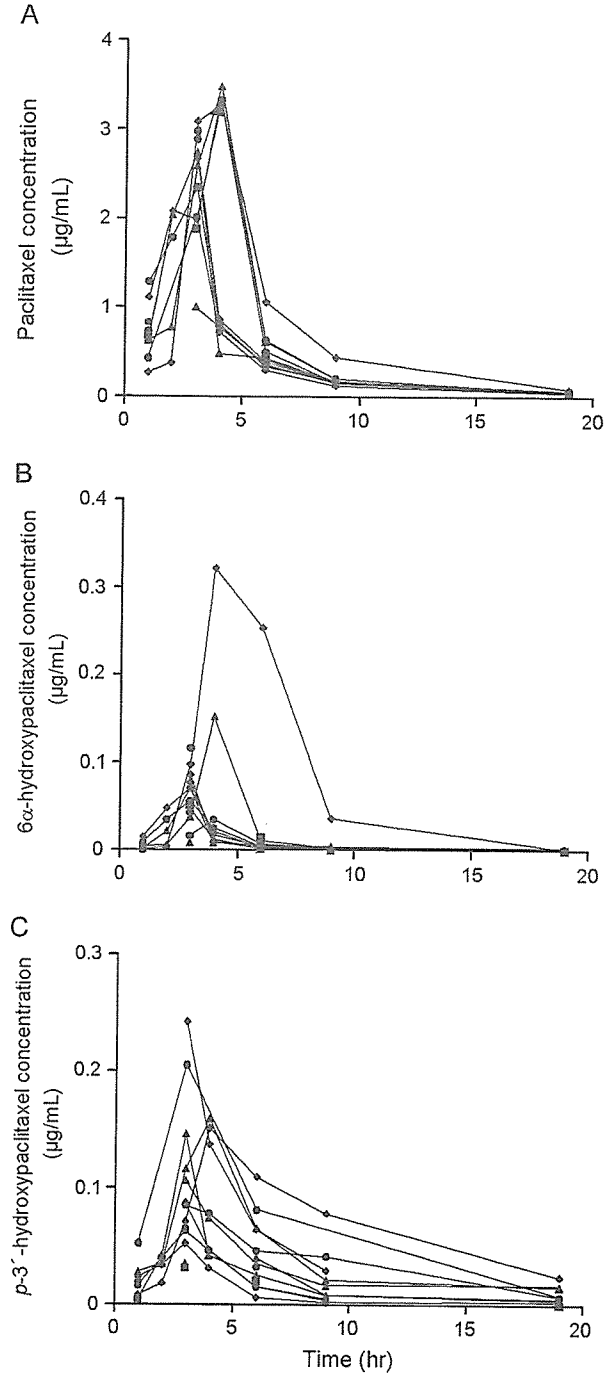

Figure 1. Plasma concentration–time curves for A) paclitaxel, B) 6α-hydroxypaclitaxel, and C) *p*-3′-hydroxypaclitaxel. Paclitaxel was administered intravenously in a 3-h infusion at a dose of approximately 175 mg/m^2. Plasma samples were obtained from 1–19 h after the start of the infusion in four to seven time points, as shown in Table 1.

Table 4. Summary of pharmacokinetic parameters ($n = 13$)

Parameter	Mean ± SD	Range
Paclitaxel		
C_{max} (μg/mL)	2.59 ± 0.67	1.00–3.46
AUC (μg·h/mL)	10.3 ± 2.47	5.7–15.0
MRT (h)	5.2 ± 0.7	4.3–6.2
V_{dss} (L/m^2)	96 ± 34	61–190
CL_{tot} (mL/min/m^2)	303 ± 767	215–499
6α-hydroxypaclitaxel		
AUC (μg·h/mL)	0.29 ± 0.36	0.09–1.47
p-3′-hydroxypaclitaxel		
AUC (μg·h/mL)	0.63 ± 0.42	0.18–1.42
AUC ratios		
6α-hydroxypaclitaxel/ *p*-3′-hydroxypaclitaxel	0.51 ± 0.33	0.13–1.03
6α-hydroxypaclitaxel/ paclitaxel	2.55 ± 2.25	0.78–9.80
p-3′-hydroxypaclitaxel/ paclitaxel	5.8 ± 3.1	2.2–10.9

MRT, mean residence time.

G2677(A,T) mutant allele had lower levels of paclitaxel AUC (10.9 ± 2.38, 11.1 ± 2.21, 5.73, 8.26, and 9.14 μg·h/mL for the 2677G/G, G/T, A/A, T/T, and A/T genotypes ([$n = 3$, 7, 1, 1, and 1], respectively). In contrast, there was no difference in the paclitaxel AUC values between the different *ABCB1* C3435T genotypes (9.79 ± 2.73, 10.9 ± 2.42, and 8.26 μg·h/mL for 3435C/C, C/T, and T/T genotypes [$n = 5$, 7, and 1], respectively).

As *ABCB1* T-129C, T1236C, and G2677(A,T) were associated with lower paclitaxel AUC (Fig. 2), we examined the relationships between total *ABCB1* mutant allele numbers and either paclitaxel AUC or CL_{tot} in 13 patients. We observed a significant correlation between paclitaxel AUC ($r = -0.721$, $P < 0.05$) and CL_{tot} ($r = 0.673$, $P < 0.05$) with *ABCB1* mutant allele dosage.

Mean paclitaxel AUC were 10.7 ± 2.30, 9.07 ± 2.95, and 12.0 μg·h/mL for *PXR* -25385C/C, C/T, and T/T ($n = 8$, 4, and 1), respectively. We also determined the 6α-hydroxypaclitaxel/paclitaxel (×100) AUC ratios (3.09 ± 2.75, 1.93 ± 0.56, and 0.78) and the *p*-3′-hydroxypaclitaxel/paclitaxel (×100) AUC ratios (6.92 ± 3.27, 3.56 ± 1.56, and 6.06) for the *PXR*-25385C/C, C/T, and T/T genotypes, respectively. There were no obvious trends in any of these parameters for the *PXR* C-25385T genotypes.

Discussion

This study sought to evaluate the effect of genetic polymorphisms within the coding sequences of proteins involved in paclitaxel elimination to the interindividual differences in paclitaxel exposure. As we observed significant interindividual variability in paclitaxel pharmacokinetics, we explored the reasons underlying this variability.

*CYP2C8*2*, *CYP2C8*3*, *CYP2C8*4*, and C1210G exhibit decreased activity against paclitaxel 6α-hydroxylase *in vitro*[15,16,22,23]. In contrast, *CYP2C8*3* was associated with reduced plasma concentrations of the CYP2C8 substrate repaglinide *in vivo*[24]. The *CYP2C8*5* mutation would be expected to cause several significant amino acid alterations and an early stop codon (http://www.imm.ki.se/CYPalleles/). Although these polymorphisms are expected to affect paclitaxel metabolism, we could not directly examine their influences on paclitaxel metabolism as no *CYP2C8* mutant alleles were detected in any of our patients. This result is consistent with another study reporting these polymorphisms to be rare in the Japanese population[22]. Thus, pharmacokinetic abnormalities in paclitaxel metabolized resulting from *CYP2C8* polymorphisms are likely rare in the Japanese.

The *CYP3A5*3* allele leads to alternative splicing that results in a truncated protein product. This is the most common cause of loss of hepatic CYP3A5 expression[10]. *CYP3A5*3*, which is common in Japanese, may account for the wide variation observed in overall CYP3A activity[25]. In our study, however, paclitaxel metabolism was not affected by the presence of

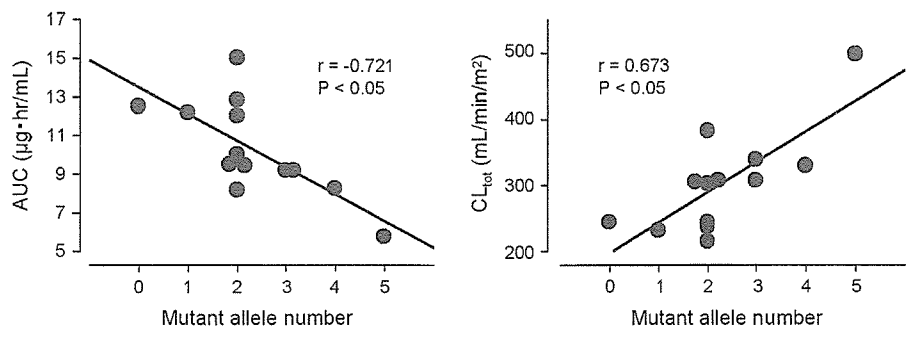

Figure 2. Correlations between paclitaxel AUC and *ABCB1* mutant allele dosage A) and between paclitaxel CL_{tot} and *ABCB1* mutant allele dosage B) in 13 patients treated with a 3-h infusion of paclitaxel. Correlations were analyzed by the Spearman rank order correlation coefficient.

the *CYP3A5*3* allele. This finding is consistent with previous reports, demonstrating that paclitaxel is a substrate for CYP3A4 but not for CYP3A5.

Increasing numbers of reports have correlated *ABCB1* genotype and phenotype with individual variations in drug efficacy. The *ABCB1* T-129C allele affects placental ABCB1 expression[17]. *ABCB1* T1236C is associated with significantly increased exposure to irinotecan and the active metabolite SN-38[26]. The *ABCB1* G2677(A,T) allele exhibits altered ABCB1 function in humans, evidenced by studies using the drug fexofenadine as a probe[27]. *ABCB1* C3435T also influences ABCB1 expression and function[28]. In this study, we demonstrated that patients with the *ABCB1* T-129C, 1236C, and 2677(A,T) alleles displayed lower paclitaxel AUC than subjects with the wild-type allele. We also observed significant correlations between both paclitaxel AUC and CL_{tot} with *ABCB1* mutant allele dosage. These results suggest that *ABCB1* polymorphisms are associated with increased clearance and decreased AUC of paclitaxel. *ABCB1* mutant alleles may be associated with higher membrane transport activity, resulting in increased clearance of paclitaxel by either increased billiary excretion or reduced enterohepatic reabsorption from the gut. Nakajima *et al.*[29] recently reported that ovarian cancer patients possessing the *ABCB1* 3435T allele had higher AUC of *p*-3′-hydroxypaclitaxel compared with those possessing the 3435C allele. They discussed that *p*-3′-hydroxypaclitaxel might be a substrate for ABCB1 with higher affinity rather than paclitaxel. Although we could not get same results (data not shown), it might be due to the different concomitant medication. The *ABCB1* phenotype has a powerful influence on both paclitaxel responses and overall survival[30], suggesting that *ABCB1* single nucleotide polymorphisms (SNPs) may also have influence on patients responses and survival following paclitaxel treatment.

Several SNPs within the PXR promoter correlated with either enhanced or reduced expression of target genes[21]. Of these SNPs, the mutation in the *PXR* C-25385T allele lies within the consensus elements for nuclear factor–kappa B and interferon stimulated gene factor–3 binding. This mutation is the most frequent SNP in Caucasians and African Americans, suggesting that this SNP may also affect paclitaxel metabolism and excretion mediated by CYP2C8, CYP3A4, and ABCB1 in Japanese patients. Our correlational study, however, demonstrates that *PXR* C-25385T did not alter paclitaxel clearance. It will be important to confirm this result and other PXR phenotypic associations in an expanded patient population.

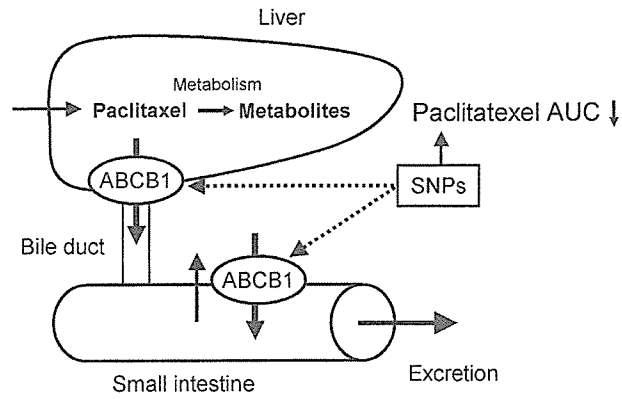

Figure 3. Scheme of proposed effect of *ABCB1* SNPs on paclitaxel disposition.

In conclusion, it may be possible to predict paclitaxel pharmacokinetics by *ABCB1* genotyping (Fig. 3). Although the *ABCB1* polymorphisms analyzed in this study cannot completely account for the differences in paclitaxel pharmacokinetics observed among patients, ABCB1 genotyping may contribute to the achievement of individualized treatment strategies with paclitaxel. Larger comprehensive studies examining the correlations between paclitaxel pharmacokinetics and genetic polymorphisms will be necessary to predict and adjust paclitaxel treatment regimens.

Acknowledgment

This research was supported by a grant from the Ministry of Education, Culture, Sports, Science and Technology and by a research grant from the Uehara Memorial Foundation.

References

1 Rowinsky EK. The development and clinical utility of the taxane class of antimicrotubule chemotherapy agents. *Annu Rev Med* 1997; 48:353–74.
2 Wiernik PH, Schwartz EL, Strauman JJ, Dutcher JP, Lipton RB, Paietta E. Phase I clinical and pharmacokinetic study of taxol. *Cancer Res* 1987;47:2486–93.
3 Brown T, Havlin K, Weiss G *et al.* A phase I trial of taxol given by a 6-hour intravenous infusion. *J Clin Oncol* 1991;9:1261–7.
4 Grem JL, Tutsch KD, Simon KJ *et al.* Phase I study of taxol administered as a short i.v. infusion daily for 5 days. *Cancer Treat Rep* 1987;71:1179–84.
5 Longnecker SM, Donehower RC, Cates AE *et al.* High-performance liquid chromatographic assay for taxol in human plasma and urine and pharmacokinetics in a phase I trial. *Cancer Treat Rep* 1987;71: 53–9.
6 Walle T, Walle UK, Kumar GN, Bhalla KN. Taxol metabolism and disposition in cancer patients. *Drug Metab Dispos* 1995;23:506–12.
7 Cresteil T, Monsarrat B, Alvinerie P, Treluyer JM, Vieira I, Wright M. Taxol metabolism by human liver microsomes: identification of cytochrome P450 isozymes involved in its biotransformation. *Cancer Res* 1994;54:386–92.

8 Rahman A, Korzekwa KR, Grogan J, Gonzalez FJ, Harris JW. Selective biotransformation of taxol to 6 alpha-hydroxytaxol by human cytochrome P450 2C8. *Cancer Res* 1994;**54:**5543–6.
9 Harris JW, Rahman A, Kim BR, Guengerich FP, Collins JM. Metabolism of taxol by human hepatic microsomes and liver slices: participation of cytochrome P450 3A4 and an unknown P450 enzyme. *Cancer Res* 1994;**54:**4026–35.
10 Kuehl P, Zhang J, Lin Y *et al.* Sequence diversity in CYP3A promoters and characterization of the genetic basis of polymorphic CYP3A5 expression. *Nat Genet* 2001;**27:**383–91.
11 Bradley G, Ling V. P-glycoprotein, multidrug resistance and tumor progression. *Cancer Metastasis Rev* 1994;**13:**223–33.
12 Gottesman MM, Pastan I. Biochemistry of multidrug resistance mediated by the multidrug transporter. *Annu Rev Biochem* 1993;**62:**385–427.
13 Thiebaut F, Tsuruo T, Hamada H, Gottesman MM, Pastan I, Willingham MC. Cellular localization of the multidrug-resistance gene product P-glycoprotein in normal human tissues. *Proc Natl Acad Sci U S A* 1987;**84:**7735–8.
14 Xie W, Evans RM. Orphan nuclear receptors: the exotics of xenobiotics. *J Biol Chem* 2001;**276:**37739–42.
15 Bahadur N, Leathart JB, Mutch E *et al.* CYP2C8 polymorphisms in Caucasians and their relationship with paclitaxel 6alpha-hydroxylase activity in human liver microsomes. *Biochem Pharmacol* 2002; **64:**1579–89.
16 Dai D, Zeldin DC, Blaisdell JA *et al.* Polymorphisms in human CYP2C8 decrease metabolism of the anticancer drug paclitaxel and arachidonic acid. *Pharmacogenetics* 2001;**11:**597–607.
17 Tanabe M, Ieiri I, Nagata N *et al.* Expression of P-glycoprotein in human placenta: relation to genetic polymorphism of the multidrug resistance (MDR)-1 gene. *J Pharmacol Exp Ther* 2001;**297:**1137–43.
18 Hiratsuka M, Agatsuma Y, Mizugaki M. Rapid detection of CYP2C9*3 alleles by real-time fluorescence PCR based on SYBR Green. *Mol Genet Metab* 1999;**68:**357–62.
19 Jamis-Dow CA, Klecker RW, Sarosy G, Reed E, Collins JM. Steady-state plasma concentrations and effects of taxol for a 250 mg/m2 dose in combination with granulocyte-colony stimulating factor in patients with ovarian cancer. *Cancer Chemother Pharmacol* 1993;**33:** 48–52.
20 Yamaoka K, Nakagawa T, Uno T. Statistical moments in pharmacokinetics. *J Pharmacokinet Biopharm* 1978;**6:**547–58.
21 Zhang J, Kuehl P, Green ED *et al.* The human pregnane X receptor: genomic structure and identification and functional characterization of natural allelic variants. *Pharmacogenetics* 2001;**11:**555–72.
22 Nakajima M, Fujiki Y, Noda K *et al.* Genetic polymorphisms of CYP2C8 in Japanese population. *Drug Metab Dispos* 2003;**31:** 687–90.
23 Soyama A, Saito Y, Hanioka N *et al.* Non-synonymous single nucleotide alterations found in the CYP2C8 gene result in reduced in vitro paclitaxel metabolism. *Biol Pharm Bull* 2001;**24:**1427–30.
24 Niemi M, Leathart JB, Neuvonen M, Backman JT, Daly AK, Neuvonen PJ. Polymorphism in CYP2C8 is associated with reduced plasma concentrations of repaglinide. *Clin Pharmacol Ther* 2003;**74:**380–7.
25 Fukuen S, Fukuda T, Maune H *et al.* Novel detection assay by PCR-RFLP and frequency of the CYP3A5 SNPs, CYP3A5*3 and *6, in a Japanese population. *Pharmacogenetics* 2002;**12:**331–4.
26 Mathijssen RH, Marsh S, Karlsson MO *et al.* Irinotecan pathway genotype analysis to predict pharmacokinetics. *Clin Cancer Res* 2003;**9:**3246–53.
27 Kim RB, Leake BF, Choo EF *et al.* Identification of functionally variant MDR1 alleles among European Americans and African Americans. *Clin Pharmacol Ther* 2001;**70:**189–99.
28 Hoffmeyer S, Burk O, von Richter O *et al.* Functional polymorphisms of the human multidrug-resistance gene: multiple sequence variations and correlation of one allele with P-glycoprotein expression and activity in vivo. *Proc Natl Acad Sci U S A* 2000; **97:**3473–8.
29 Nakajima M, Fujiki Y, Kyo S *et al.* Pharmacokinetics of paclitaxel in ovarian cancer patients and genetic polymorphisms of CYP2C8, CYP3A4, and MDR1. *J Clin Pharmacol* 2005;**45:**674–82.
30 Penson RT, Oliva E, Skates SJ *et al.* Expression of multidrug resistance-1 protein inversely correlates with paclitaxel response and survival in ovarian cancer patients: a study in serial samples. *Gynecol Oncol* 2004;**93:**98–106.

Accepted for publication December 14, 2005